Surface properties of O2-plasma-treated thermoplastic fluoroelastomers under mechanical stretching

Urushihara, Yoshimasa

Nishino, Takashi

(Citation)
Polymer,50(14):3245-3249

(Issue Date)
2009-07-03

(Resource Type)
journal article

(Version)
Accepted Manuscript

(URL)
https://hdl.handle.net/20.500.14094/90000992

Surface Properties of O_2-plasma-treated Thermoplastic Fluoroelastomers under Mechanical Stretching

Yoshimasa Urushihara[1, 2] and Takashi Nishino[1]*

[1] Department of Chemical Science and Engineering, Graduate School of Engineering, Kobe University, Rokko, Nada, Kobe 657-8501, Japan

[2] Hyogo Science and Technology Association, 1-490-2 Kouto, Shingu-cho, Tatsuno, Hyogo 679-5165, Japan

* To whom correspondence should be addressed. Tel: +81-78-803-6164, Fax: +81-78-803-6198, E-mail: tnishino@kobe-u.ac.jp

ABSTRACT

Surface properties and structure of an oxygen-plasma-treated thermoplastic fluoroelastomer film under mechanical stretching were investigated using dynamic contact angle, X-ray photoelectron spectroscopy and field-emission scanning electron microscopy. The contact angle of water on the surface decreased from 96° to 36° by the plasma treatment. The contact angle increased under uniaxial stretching: the plasma-treatment effect decreased. This was considered to be due to a dilution of the plasma-oxidized chains through the surface exposure of the matrix embedded chains by stretching. In other words, under stretching, the

surface of plasma-treated films can be regarded as being chemically heterogeneous and being composed of treated and untreated parts. On the contrary, by the new surface modification procedure, *that is*, *in situ* plasma treatment under stretching, high hydrophilicity and high surface oxygen concentration were found to be maintained even at a high stretching ratio.

Keywords

Oxygen plasma treatment; Surface properties; Mechanical stretching

1. Introduction

Thermoplastic fluoroelastomers (TPFEs) have recently attracted great interest as sealing materials in the chemical and electronics industries [1, 2]. Examples of their outstanding properties are water- and oil-repellencies, low dielectric constant, high heat-resistance, and excellent chemical resistance. They are based on fluorocarbon characteristics as well as high rubber elasticity, and excellent processability due to their thermoplasticity. However, TPFEs possess a disadvantage in adhesion because of the lack of polar functionality on the surface, which results in poor wettability and weak interfacial interactions with other materials.

Many modification techniques have been proposed to give new properties to elastomer surfaces [3-10]. Plasma treatment is one of the most common dry techniques to modify surface wettability because it is adaptable to various shapes, *i.e.* powder, fiber, film and block. Using plasma treatments with O_2, NH_3, N_2, Ar, and CO_2 gases, polar functional groups can be introduced onto the material surfaces, which significantly increase the hydrophilicity of the surface [3, 4, 11-27]. However, a better understanding of the relationship between the deformation and the surface properties of the plasma-treated materials is needed, especially for elastomers. This is because elastomeric materials are often used under large stretching

and the treatment effect is thought to be affected by the stretching.

In this study, TPFE was chosen as a starting material because large differences of the surface properties will be expected before and after O_2 plasma treatment. A change in wettability of an O_2-plasma-treated TPFE film was investigated under uniaxial stretching. We proposed a new surface modification procedure to maintain high surface hydrophilicity even at a high stretching ratio.

2. Experimental section

2.1. Sample preparation

The TPFE used in this study was kindly supplied from Daikin Industry Ltd., tradenamed T-530. This elastomer is a block copolymer composed of vinylidene fluoride-hexafluoropropene soft segments and ethylene-tetrafluoroethylene hard segments [1]. The TPFE film was prepared by melt-pressing with being sandwiched between polytetrafluoroethylene sheets at 5 MPa 250°C, and then gradually cooled down to room temperature over 3 h. The thickness of the TPFE film was 50 μm. The melting endotherm was observed at 238°C using a differential scanning calorimeter (DSC120, Seiko Instruments Inc.). The O_2 plasma treatment was carried out using an ULVAC EBH-6 vacuum chamber with a radio frequency (RF = 13.56 MHz) coil. The TPFE film was set at a distance of 50 mm from the RF coil and treated at the RF power of 200W for 60 s under a pressure of 0.5 Pa. Just after treatment, a 30 mm square sample was uniaxially stretched under ambient conditions. When the TPFE was stretched, the stress relaxation started to occur at any strains. So, the stretched samples were left for more than 30 min at each fixed strain as a pre-conditioning step before the measurements. Within this period, the stress relaxation apparently reached to equilibrium, then all the measurements were performed.

2.2. Contact angle measurement

Contact angle measurements were carried out by a dynamic sessile drop method using a home-made apparatus. The shapes of the liquid droplets on the samples were monitored from the side using an optical scope. The advancing contact angle θ_a was measured when the contact area between the liquid droplet and the sample surface was enlarged (< 2 mm in diameter) by increasing the droplet volume. On the other hand, the receding contact angle θ_r was measured when the contact area was reduced by decreasing the droplet volume. To estimate the average surface wettability of the sample, the average contact angle θ was calculated as

$$\theta = \cos^{-1}\left\{\left(1/2\right)\cdot\left(\cos\theta_a + \cos\theta_r\right)\right\}. \quad (1)$$

The contact angle data for each sample were reproducible, and the experimental errors of the θ values were evaluated to be less than ±2°.

2.3. X-ray photoelectron spectroscopy (XPS)

XPS measurements were carried out using a Shimadzu ESCA-850 to investigate the surface atomic ratio between oxygen and carbon. The samples were irradiated with MgKα radiation generated at 8 kV and 30 mA, then the XPS spectra were collected at 15°, 30°, 45°, 60° and 90° of the photoelectron take-off angle γ between the sample and the analyzer. The analytical depth could be decreased by decreasing γ. The pressure in the instrumental chamber was less than 1.0 x 10^{-5} Pa. For the XPS measurements under uniaxial stretching, the stretched sample was fixed to an aluminium plate using cyanoacrylate type adhesive.

2.4. Field-emission scanning electron microscopy (FE-SEM)

The morphological changes of the sample surface by stretching were observed using a FE-SEM (JEOL, JSM-7401F) equipped with a stretching device for an uniaxial tensile test (Sanyu electron, SS-7200L) [28]. Since the TPFE is a non-conducting material, the charge-up of the surface causes the severe degradation of the images. Carbon and metal coatings onto the sample surface have been often performed to prevent the charge-up. These coatings, however, were ruptured by stretching, which may give us the incorrect images of the sample surface. So, low accelerating voltage and low dose methods [29] were employed to prevent the image degradation due to the charge-up in this study. FE-SEM was operated at acceleration voltage of 1.0 kV and electron probe current of 3 pA.

3. Results and Discussion

Figure 1 shows the relationship between strain ε by uniaxial stretching/recovering and contact angle θ on the as-melt-pressed and the O_2-plasma-treated TPFE surface. The TPFE films were uniaxially stretched up to ε = 200% and then allowed to recover, which was repeated twice. The θ value of the TPFE film drastically dropped from 96° to 36° by the O_2 plasma treatment. The O_2-plasma-treated film showed that the θ value increased from 36° to 69° with increasing ε. Whereas, the θ value of the as-melt-pressed TPFE film was intrinsically invariant with respect to the stretching. Though *ca.* 15% of the residual strain existed after recovering from 200%-stretching, the changes in the θ value were reversible within these stretching/recovering cycles.

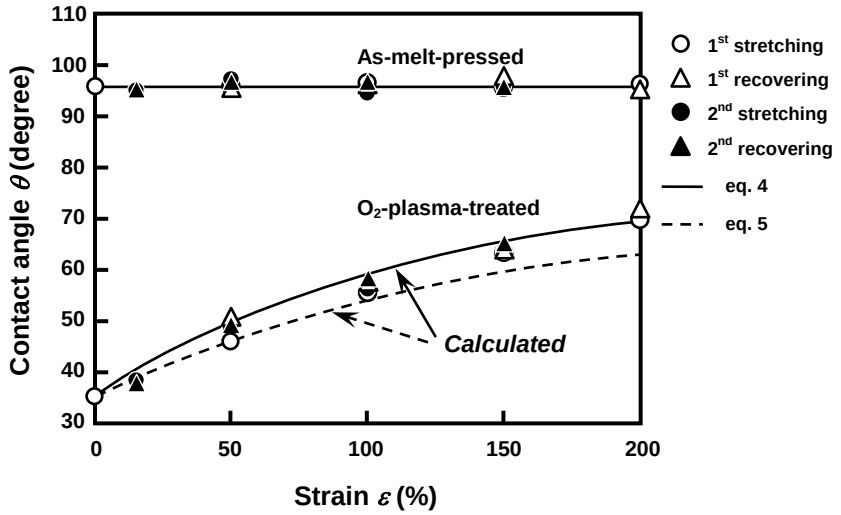

Figure 1 Effect of strain ε by uniaxial stretching/recovering on contact angle of water for the as-melt-pressed and the O_2-plasma-treated TPFE film. The TPFE film was O_2-plasma treated at the RF power of 200 W for 60 s.

Figure 2 shows the relationship between the strain ε by uniaxial stretching and the macroscopic surface area ratio S/S_0 of the TPFE film. S_0 and S are the surface area before and under stretching, respectively. The S/S_0 ratio was evaluated from the deformation of a 10 mm square area at the center of the film surface. The S/S_0 ratio showed a linear relation to the strain ε, which could be fitted to the following equation using the linear least-square method;

$$S(\varepsilon)/S_0 = 0.43\times10^{-2}\cdot\varepsilon(\%)+1. \qquad (2)$$

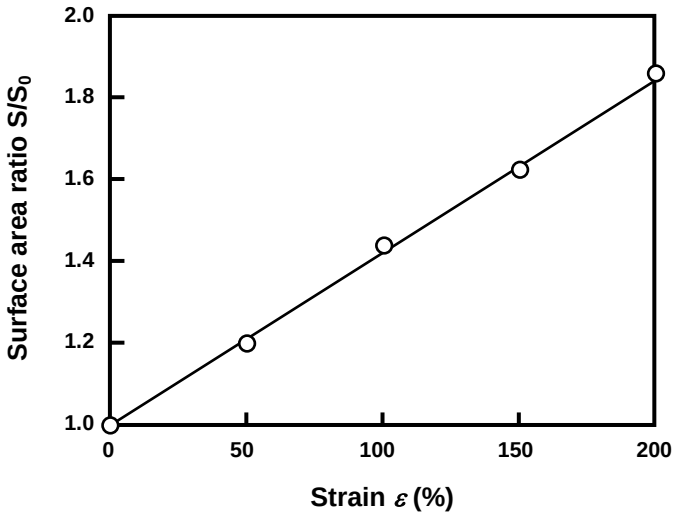

Figure 2 Relationship between strain ε by uniaxial stretching and macroscopic surface area ratio S/S_0 of the TPFE film. S_0 and S are the surface area before and under uniaxial stretching.

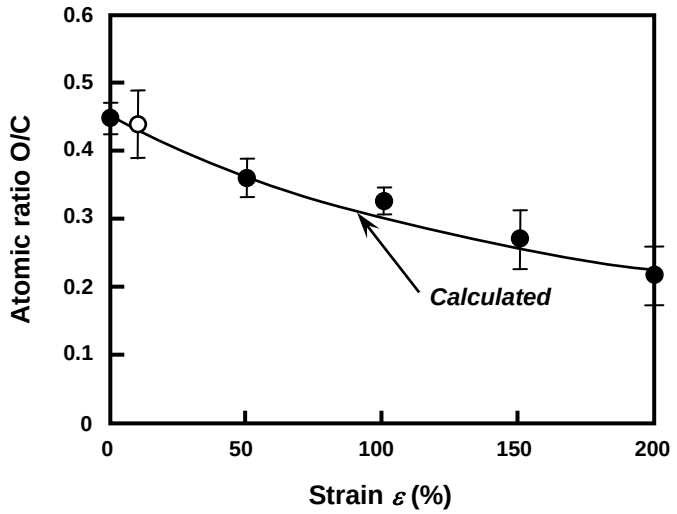

Figure 3 Effect of strain ε by uniaxial stretching on atomic ratio O/C collected at take-off angle γ of 15° of the O_2-plasma-treated TPFE film. The O/C value of the O_2-plasma-treated film recovered from 200%-stretching was superimposed with open circle. The TPFE film was O_2-plasma treated at the RF power of 200 W for 60 s.

Figure 3 shows the effect of strain ε by uniaxial stretching on the O/C atomic ratio of the O_2-plasma-treated TPFE film. The O/C value of the film after recovered from 200%-stretching was superimposed with an open circle. The solid curve in the figure reveals the calculated results using the following equation;

$$O/C \text{ at a ceratin } \varepsilon \;=\; \frac{O/C \text{ at the initial condition}}{S(\varepsilon)/S_0}. \qquad (3)$$

Eq.3 was based on the idea: the O/C value decreases to half of that at the initial condition, when the surface area doubles ($S/S_0 = 2$). Here, an O/C value of 0.45 was used as that at the initial condition, and the $S(\varepsilon)/S_0$ expressed by eq. 2 was used for the calculation. The experimental O/C values coincided well with the calculated curve as shown in the figure. This indicates that a change in the surface oxygen concentration directly relates to a change in the surface area.

Next, we assumed that the O_2-plasma-treated TPFE surface under uniaxial stretching was composed of the two different parts, α: the plasma-treated part and β: the untreated TPFE part exposed from the bulk to the surface by stretching. Several equations have been proposed to describe the relationship between the contact angles and the heterogeneous surface composed of the two parts [4, 30-33]. The Cassie equation (eq.4) [30] and the Israelachvili equation (eq.5) [33] were both used in this study.

$$\cos\theta = f_\alpha \cos\theta_\alpha + f_\beta \cos\theta_\beta \qquad (4)$$

and

$$(1+\cos\theta)^2 = f_\alpha (1+\cos\theta_\alpha)^2 + f_\beta (1+\cos\theta_\beta)^2, \qquad (5)$$

where f_α and f_β ($f_\alpha + f_\beta = 1$) were the area fractions of the heterogeneous surface. Here, θ_α = 36° and θ_β = 96° were used as the contact angles on the plasma-treated part and the untreated

TPFE part, respectively. The curves calculated from eq. 4 and 5 are drawn with the solid and broken lines in Fig. 1, respectively. The calculated curves were very similar to the experimental data. These results suggest that the surface of the O_2-plasma treated TPFE film can be regarded as being chemically heterogeneous under uniaxial stretching.

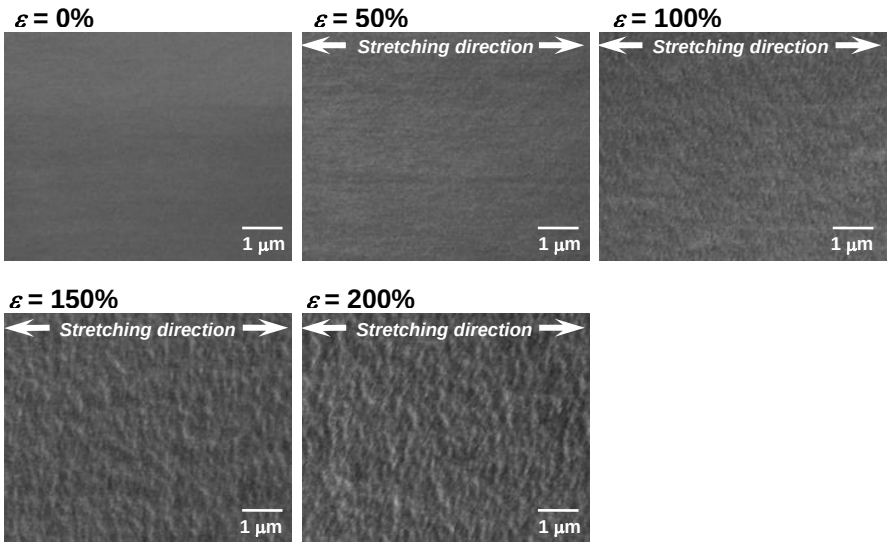

Figure 4 FE-SEM images of O_2-plasma-treated TPFE film before and under stretching at ε = 50%, 100%, 150% and 200%. The TPFE film was O_2-plasma treated at the RF power of 200 W for 60 s.

Figure 4 shows the FE-SEM images of the O_2-plasma-treated TPFE film before and under stretching at ε = 50%, 100%, 150% and 200%. When the film was stretched, fibril-like morphology perpendicular to the stretching direction appeared. As for the surface etching effects of plasma treatments on semi-crystalline polymers, it have been reported that the amorphous regions were preferentially etched and then followed by crystalline ones [13, 20, 34]. Beake *et al*. investigated the surface morphologies of polyethylene terephthalate (PET) films treated by Ar plasma using a scanning force microscopy [34]. The surface stretched after Ar plasma treatment showed fibril-like morphology perpendicular to the stretching direction, corresponding to the alignments of lamella stacks. Nakayama *et al.* also investigated morphological changes of the Ar-plasma-treated PET films before and after

stretching using a transmission electron microscopy (TEM) [11]. The stretched PET surface could be divided into two parts, *that is*, the plasma-treated layer and the untreated PET, which were clearly observed by the TEM micrographs taken from the cross section. Their observations are similar to the feature observed on the FE-SEM images in Fig. 4. TPFE used in this study is the block copolymer which forms a microphase-separation structure composed of crystalline hard-segment domains and soft-segment phases [1]. The plasma-treated TPFE surface before stretching was thought to be covered with the hard-segment domains because of the preferential etching of the soft-segment phases. Thus, the observed fibril-like morphology under stretching will result from newly exposure of the soft-segment phases between the hard-segment domains. Here, the ridge and ditch parts of the fibril-like morphology correspond to the plasma-treated hard-segment domain and the newly exposed soft-segment phase, respectively. The surface exposure of the embedded soft-segment phases by stretching caused a decrease in the apparent oxygen concentration, which results in an increase in the contact angle under stretching on the plasma-treated film surface.

Based on the information shown above, the hydrophilicity of the O_2-plasma-treated TPFE film is expected to be increased by increasing the surface oxygen concentration using the treatment procedure as schematically shown in Figure 5. Hereafter, we call this procedure as the PsPR (Pre-stretching followed by Plasma treatment *in situ* under stretching and then allowed to Recover).

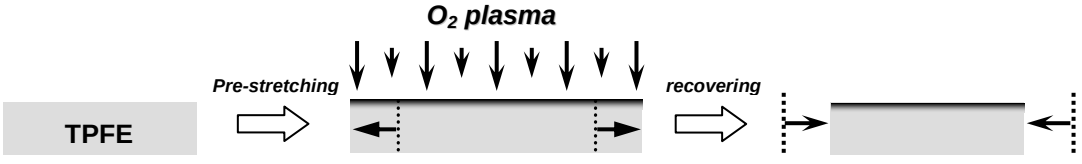

Figure 5 Schematic illustration of O_2-plasma-treatment procedure; Pre-stretching - Plasma treatment - Recovering (PsPR).

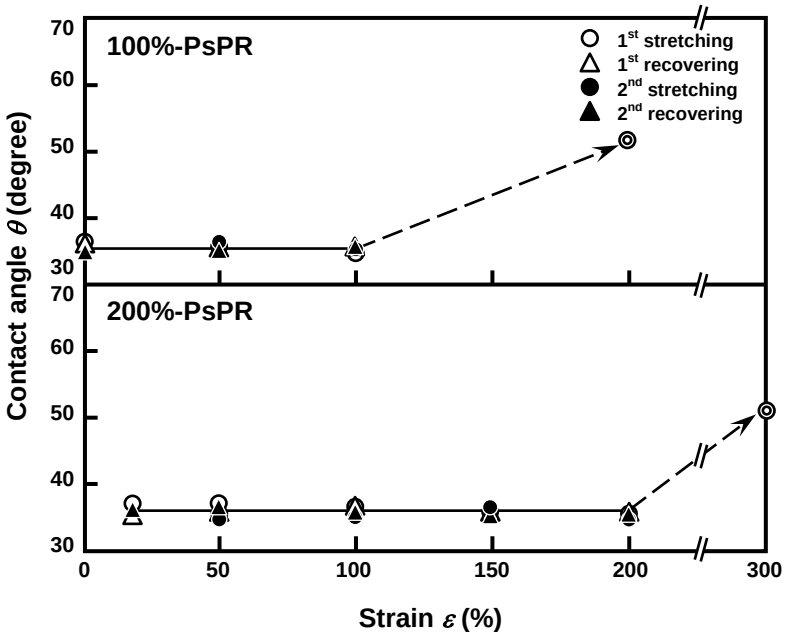

Figure 6 Effect of strain ε by uniaxial stretching on contact angle of water on 0%-, 100%-, and 200%-PsPR films. The TPFE films were O_2-plasma treated at the RF power of 200 W for 60 s.

Figure 6 shows the relationship between strain ε by uniaxial stretching/recovering and the contact angle on the TPFE films surface treated by PsPR procedure. The 200%-PsPR film means that the film was *in situ* plasma-treated at the pre-stretching strain ζ = 200% and then recovered. The 100%- and 200%-PsPR films possessed the same contact angle (*ca.* θ = 36°) after the PsPR procedure, which also coincides with the θ value for the film without PsPR procedure, the 0%-PsPR film, in Fig. 1. As described before, the θ value increased with increasing ε for the 0%-PsPR film. On the contrary, the θ values of the 100%- and the 200%-PsPR films remained unchanged as long as the stretching strain ε did not exceed each pre-stretching strain ζ. In addition, their low θ values were reversible during the stretching/recovering cycles. After the ε value exceeded each ζ, the θ value increased as indicated by double circles in the figure.

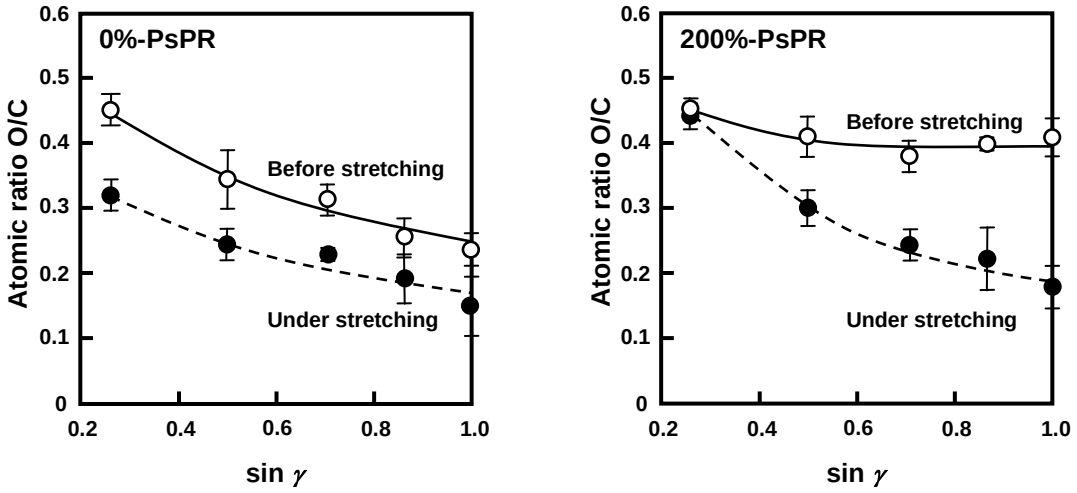

Figure 7 Angular-dependence of atomic ratios O/C for 0%- and 200%-PsPR films before and under uniaxial stretching. The 0%- and the 200%-PsPR films were stretched at ε = 100% and ε = 200%, respectively. The TPFE films were O_2-plasma treated at the RF power of 200 W for 60 s.

Figure 7 shows the angular-dependence of the atomic ratio O/C of the 200%-PsPR film before and under uniaxial stretching at ε = 200% together with the results for the 0%-PsPR film before and under uniaxial stretching at ε = 100%. The 0%-PsPR film under stretching showed a lower oxygen concentration for all analytical depths than that before stretching. On the contrary, the oxygen concentration was kept high for the 200%-PsPR film before stretching even at sinγ of 1.0 (γ = 90°), although that under stretching gradually decreased with increasing the analytical depth. In addition, the O/C values at the uppermost surface (the take-off angle γ = 15°) was unchanged before and under stretching, which supports the constant contact angle up to ε = 200% shown in the bottom figure of Fig. 6. These results indicate that the thicker plasma-treated layer was formed on the 200%-PsPR film, and the stretching/recovering process only changed the thickness of the plasma-modified layer.

Summarizing the information shown above, possible structural models of the 0%- and the 200%-PsPR film surfaces could be schematically illustrated in Figure 8. Since the surface area of the film increased by the surface exposure of the embedded TPFE chains in the matrix

under uniaxial stretching, the 0%-PsPR film would possess a heterogeneous surface morphology composed of the plasma-treated and the freshly exposed TPFE parts (Fig. 8 a). The surface exposure of the untreated TPFE chains caused a decrease in the surface oxygen concentration, which resulted in an increase of the contact angle under uniaxial stretching. On the other hand, by treating the film with the plasma at ζ = 200%, the thickness of the treated layer apparently increased after recovering, so that the film surface might be completely covered with the treated layer even under uniaxial stretching. This results in a very low contact angle even under uniaxial stretching to the 200%-PsPR film (Fig. 8 b).

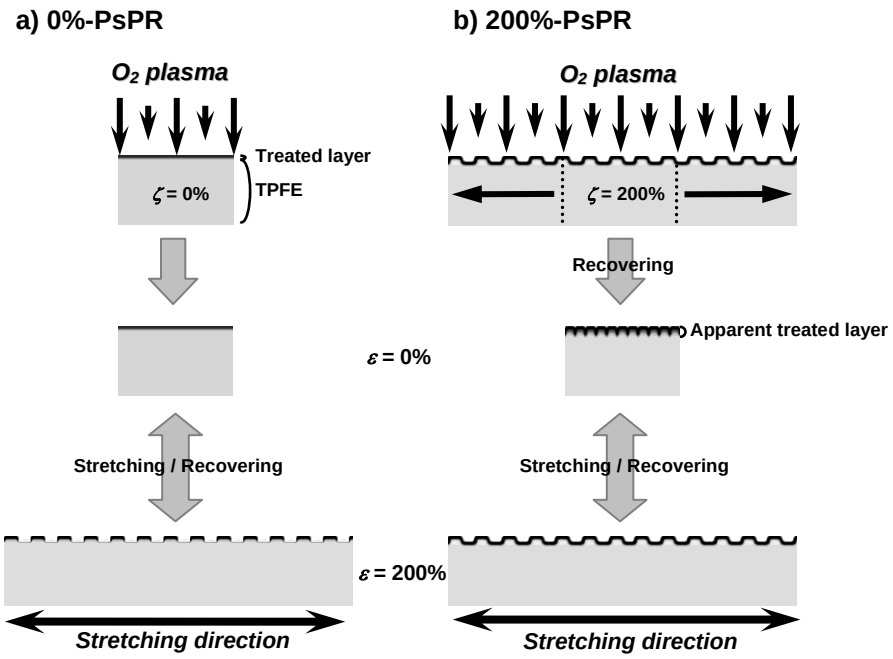

Figure 8 Schematic illustrations of surface structures of a) 0%- and b) 200%-PsPR films before and under uniaxial stretching.

Conclusions

The surface properties and structures of the O_2-plasma-treated TPFE under uniaxial stretching were investigated. The TPFE is very hydrophobic (θ = 96°), but it turned hydrophilic (θ = 36°) after plasma treatment. The contact angle was found to decrease by tensile deformation, but recovered after releasing the applied strain. This phenomenon was reversible for the stretching/recovering process, which was explained by a change in surface concentration of the polar functional groups. These findings suggest that the embedded TPFE chains in the bulk were exposed to the surface by stretching the film. By using the PsPR procedure, a thick plasma-modified layer was formed. The high hydrophilic surface was maintained during the stretching/recovering process. The experimental results show that this PsPR procedure was useful to produce the high performance surfaces of the rubber materials.

Acknowledgement

The authors acknowledge Daikin Industry Ltd. for supplying of thermoplastic fluoroelastomer. Eno Fundation and Special Coordination Funds for Promoting Science and Technology, Creation of Innovation Centers for Advanced Interdisciplinary Research Areas (Innovative Bioproduction Kobe), MEXT, Japan are also acknowledged for financial support. This study has been carried out through Collaboration of Regional Entities for the Advancement of Technological Excellence organized by HYOGO Prefecture and funded by the Japan Science and Technology Agency.

Reference

1. Tatemoto M, Shimizu T. Fluorinated Thermoplastic Elastomers. In: Scherirs J, editor. Modern Fluoropolymers: High Performance Polymers for Diverse Applications. Chichester: John Wiley & Sons, 1997. pp. 565-576.

2. Ameduri B, Boutevin B. Well-architectured Fluoropolymers: Synthesis, Properties and Applications. Amsterdam: Elsevier, 2004.

3. Feast WJ, Munro HS, Richards RW, editors. Polymer Surface and Interface II. Chichester: Wiley, 1993.

4. Garbassi F, Morra M, Occhiello E. Polymer Surface: From Physics to Technology. Chichester: John Wiley & Sons, 1998.

5. Ouyang M, Yuan C, Muisener RJ, Boulares A, Koberstein JT. Chem Matter 2000; 12: 1591-1596.

6. Kim J, Chaudhury MK, Owen MJ, Orbeck T. J Colloid Interface Sci 2001; 244: 200-207.

7. Truica-Marasescu F, Jedrzejowski P, Wertheimer MR. Plasma Proc Polym 2004; 1: 153-163.

8. Oláh A, Hillborg H, Vancso GJ. Appl Surf Sci 2005; 239: 410-423.

9. Waddel EA, Shreeves S, Carrell H, Perry C, Reid BA, McKee J. Appl Surf Sci 2008; 254: 5314-5318.

10. O'Connell C, Sherlock R, Ball MD, Aszalós-kiss B, Prendergast U, Glynn TJ. Appl Surf Sci 2009; 255: 4405-4413.

11. Nakayama Y, Soeda F, Ishitani A. Polym Eng Sci 1991; 31: 812-817.

12. Terlingen GAJ, Takens GAJ, van der Gaag FJ, Hoffman AS, Feijen J. J Appl Polym Sci 1994; 52: 39-53.

13. Choi DM, Park CK, Cho K, Park CE. Polymer 1997; 38: 6243-6249.

14. Kim H, Urban MW. Langmuir 1999; 15: 3499-3505.

15. Hillborg H, Ankner JF, Gedde UW, Smith GD, Yasuda HK, Wikstöm K. Polymer 2000;

41: 6851-6863.

16. Hyum J. Polymer 2001; 42: 6473-6477.

17. Legonkova OA, Chalykh AE, Ananiev VV. Polym Plast Technol Eng 2002; 41: 489-501.

18. Park YW, Inagaki N. Polymer 2003; 44: 1569-1575.

19. Kim KS, Ryu CM, Park CS, Sur GS, Park CE. Polymer 2003; 44: 6287-6295.

20. Ginn BT, Steinbock O. Langmuir 2003; 19: 8117-8118.

21. Kaplan S. Surf Coat Tech 2004; 186: 214-217.

22. Williams RL, Wilson DJ, Rhodes NP. Biomaterials 2004; 25: 4659-4673.

23. Meincken M, Berhane TA, Mallon PE. Polymer 2005; 46: 203-208.

24. Dai C-A, Lee Y-H, Chui A-C, Tsui T-A, Lin K-J, Chen K-L, Liu M-W. Polymer 2006; 47: 8583-8594.

25. Švorčík V, Kolářová K, Slepička P, Macková A, Novotná M, Hnatowicz V. Polym Deg Stab 2006; 91: 1219-1225.

26. Bodas D, Khan-Malek C. Sens Actuators B 2007; 123: 368-373.

27. Bodas D, Rauch JY, Khan-Malek C. Euro Poly J 2008; 44: 2130-2139.

28. Urushihara Y, Li L, Matsui J, Nishino T. Composites A 2009; 40: 232-234.

29. Joseph IG, Dale EN, David CJ, Charles EL, Patric E, Eric L, Linda S, Joseph RM. Scanning Electron Microscopy and X-ray Microanalysis 3rd ed. USA: Springer, 2003.

30. Cassie ABD. Discuss Faraday Soc 1948; 3: 11–16.

31. Neumann AW, Good RJ. J Colloid Interface Sci 1972; 38: 341-358.

32. Schwartz LW, Garoff S. Langmuir 1985; 1: 219-230.

33. Israelachvili JN, Gee ML. Langmuir 1989; 5: 288-289.

34. Beake BD, Ling JSG, Leggett GJ. J Mater Chem 1998; 8: 1735-1742.